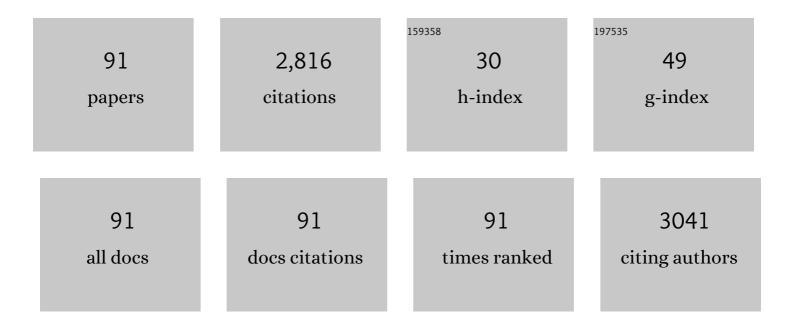
List of Publications by Year in descending order

Source: https://exaly.com/author-pdf/4887253/publications.pdf Version: 2024-02-01



#	Article	IF	CITATIONS
1	Binary Co–Ni oxide nanoparticle-loaded hierarchical graphitic porous carbon for high-performance supercapacitors. Journal of Materials Science and Technology, 2020, 37, 135-142.	5.6	140
2	Simple synthesis of graphene-doped flower-like cobalt–nickel–tungsten–boron oxides with self-oxidation for high-performance supercapacitors. Journal of Materials Chemistry A, 2017, 5, 9907-9916.	5.2	122
3	CaCl2·6H2O/Expanded graphite composite as form-stable phase change materials for thermal energy storage. Journal of Thermal Analysis and Calorimetry, 2014, 115, 111-117.	2.0	116
4	Ammonia sensor based on polypyrrole–graphene nanocomposite decorated with titania nanoparticles. Ceramics International, 2015, 41, 6432-6438.	2.3	106
5	Broccoli-like porous carbon nitride from ZIF-8 and melamine for high performance supercapacitors. Applied Surface Science, 2018, 440, 47-54.	3.1	105
6	One-pot synthesis of ternary polypyrroleâ¿¿Prussian-blueâ¿¿graphene-oxide hybrid composite as electrode material for high-performance supercapacitors. Electrochimica Acta, 2016, 188, 126-134.	2.6	104
7	Rational Design of Co(II) Dominant and Oxygen Vacancy Defective CuCo ₂ O ₄ @CQDs Hollow Spheres for Enhanced Overall Water Splitting and Supercapacitor Performance. Inorganic Chemistry, 2018, 57, 7380-7389.	1.9	104
8	Doping composite of polyaniline and reduced graphene oxide with palladium nanoparticles for room-temperature hydrogen-gas sensing. International Journal of Hydrogen Energy, 2016, 41, 5396-5404.	3.8	93
9	A room-temperature hydrogen sensor based on Pd nanoparticles doped TiO 2 nanotubes. Ceramics International, 2014, 40, 16343-16348.	2.3	89
10	Spacing graphene and Ni-Co layered double hydroxides with polypyrrole for high-performance supercapacitors. Journal of Materials Science and Technology, 2020, 55, 190-197.	5.6	79
11	Carbon dots decorated ultrathin CdS nanosheets enabling in-situ anchored Pt single atoms: A highly efficient solar-driven photocatalyst for hydrogen evolution. Applied Catalysis B: Environmental, 2019, 259, 118036.	10.8	77
12	Polydopamine-assisted formation of Co3O4-nanocube-anchored reduced graphene oxide composite for high-performance supercapacitors. Ceramics International, 2019, 45, 13894-13902.	2.3	74
13	Chitosan-mediated Co–Ce–B nanoparticles for catalyzing the hydrolysis of sodium borohydride. International Journal of Hydrogen Energy, 2018, 43, 4912-4921.	3.8	72
14	Hydrogen generation by hydrolysis of alkaline sodium borohydride using a cobalt–zinc–boron/graphene nanocomposite treated with sodium hydroxide. International Journal of Hydrogen Energy, 2015, 40, 4111-4118.	3.8	60
15	Highly active nanoporous Co–B–TiO2 framework for hydrolysis of NaBH4. Ceramics International, 2015, 41, 899-905.	2.3	56
16	Light metal borohydrides/amides combined hydrogen storage systems: composition, structure and properties. Journal of Materials Chemistry A, 2017, 5, 25112-25130.	5.2	55
17	Polypyrrole-wrapped NiCo2S4 nanoneedles as an electrode material for supercapacitor applications. Ceramics International, 2021, 47, 16562-16569.	2.3	55
18	Nitrogen-doped porous carbon derived from ginkgo leaves with remarkable supercapacitance performance. Diamond and Related Materials, 2019, 98, 107475.	1.8	49

Sнијим Qiu

#	Article	IF	CITATIONS
19	Flexible asymmetric supercapacitors made of 3D porous hierarchical CuCo2O4@CQDs and Fe2O3@CQDs with enhanced performance. Electrochimica Acta, 2018, 283, 248-259.	2.6	47
20	Ruthenium supported on nitrogen-doped porous carbon for catalytic hydrogen generation from NH3BH3 hydrolysis. International Journal of Hydrogen Energy, 2019, 44, 1774-1781.	3.8	47
21	Solvothermal synthesis of cobalt nickel layered double hydroxides with a three-dimensional nano-petal structure for high-performance supercapacitors. Sustainable Energy and Fuels, 2020, 4, 337-346.	2.5	42
22	Cobalt–boron/nickel–boron nanocomposite with improved catalytic performance for the hydrolysis of ammonia borane. International Journal of Hydrogen Energy, 2015, 40, 13423-13430.	3.8	41
23	Bienzymatic glucose biosensor based on direct electrochemistry of cytochrome c on gold nanoparticles/polyaniline nanospheres composite. Talanta, 2013, 110, 96-100.	2.9	37
24	Thermal stability, decomposition and glass transition behavior of PANI/NiO composites. Journal of Thermal Analysis and Calorimetry, 2009, 98, 533-537.	2.0	35
25	Effect of ball-milling time on the electrochemical properties of La–Mg–Ni-based hydrogen storage composite alloys. International Journal of Hydrogen Energy, 2007, 32, 4925-4932.	3.8	34
26	The improved electrochemical properties of novel La–Mg–Ni-based hydrogen storage composites. Electrochimica Acta, 2007, 52, 6700-6706.	2.6	33
27	Pd-doped TiO2@polypyrrole core-shell composites as hydrogen-sensing materials. Ceramics International, 2016, 42, 8257-8262.	2.3	33
28	Electrochemical hydrogen storage properties of La0.7Mg0.3Ni3.5–Ti0.17Zr0.08V0.35Cr0.1Ni0.3La0.7Mg0.3Ni3.5–Ti0.17Zr0.08V0.35Cr0.1Ni0.3 composites International Journal of Hydrogen Energy, 2008, 33, 755-761.	5. 3.8	32
29	Biomassâ€Derived Porous Carbon Prepared from Egg White for Highâ€performance Supercapacitor Electrode Materials. ChemistrySelect, 2019, 4, 7358-7365.	0.7	32
30	Preparation and thermophysical properties of a novel form-stable CaCl2·6H2O/sepiolite composite phase change material for latent heat storage. Journal of Thermal Analysis and Calorimetry, 2018, 131, 57-63.	2.0	31
31	Co3O4-doped two-dimensional carbon nanosheet as an electrode material for high-performance asymmetric supercapacitors. Electrochimica Acta, 2020, 335, 135611.	2.6	29
32	Two dimensional holey carbon nanosheets assisted by calcium acetate for high performance supercapacitor. Electrochimica Acta, 2018, 283, 904-913.	2.6	28
33	Poly(N-vinyl-2-pyrrolidone)-stabilized ruthenium supported on bamboo leaf-derived porous carbon for NH3BH3 hydrolysis. International Journal of Hydrogen Energy, 2019, 44, 29255-29262.	3.8	26
34	Effect of polyaniline on hydrogen absorption–desorption properties and discharge capacity of AB3 alloy. International Journal of Hydrogen Energy, 2007, 32, 3395-3401.	3.8	25
35	Rambutanâ€like hierarchically porous carbon microsphere as electrode material for highâ€performance supercapacitors. , 2021, 3, 361-374.		25
36	Ternary Co–Ni–B amorphous alloy with a superior electrochemical performance in a wide temperature range. International Journal of Hydrogen Energy, 2016, 41, 3955-3960.	3.8	24

#	Article	IF	CITATIONS
37	Thermochemical studies of Rhodamine B and Rhodamine 6G by modulated differential scanning calorimetry and thermogravimetric analysis. Journal of Thermal Analysis and Calorimetry, 2016, 123, 1611-1618.	2.0	22
38	Al–Li3AlH6: A novel composite with high activity for hydrogen generation. International Journal of Hydrogen Energy, 2014, 39, 10392-10398.	3.8	21
39	Nitrogen-doped porous microsphere carbons derived from glucose and aminourea for high-performance supercapacitors. Catalysis Today, 2018, 318, 150-156.	2.2	21
40	Nitrogen-rich sandwich-like carbon nanosheets as anodes with superior lithium storage properties. Inorganic Chemistry Frontiers, 2018, 5, 225-232.	3.0	21
41	Effect of doped Ni-Bi-B alloy on hydrogen generation performance of Al-InCl3. Journal of Energy Chemistry, 2019, 39, 268-274.	7.1	21
42	Nitrogen-doped carbon encapsulated Ru-decorated Co2P supported on graphene oxide as efficient catalysts for hydrogen generation from ammonia borane. Journal of Alloys and Compounds, 2022, 921, 166207.	2.8	21
43	Heat capacities and thermodynamic properties of CoPc and CoTMPP. Journal of Thermal Analysis and Calorimetry, 2008, 91, 841-848.	2.0	20
44	Electrochemical kinetics and its temperature dependence behaviors of Ti0.17Zr0.08V0.35Cr0.10Ni0.30 alloy electrode. Journal of Alloys and Compounds, 2009, 471, 453-456.	2.8	20
45	Cobalt-Nickel-Boron Supported over Polypyrrole-Derived Activated Carbon for Hydrolysis of Ammonia Borane. Metals, 2016, 6, 154.	1.0	20
46	Enhanced hydrogen storage properties of 2LiNH2/MgH2 through the addition of Mg(BH4)2. Journal of Alloys and Compounds, 2017, 704, 44-50.	2.8	20
47	Self-assembly synthesis of nitrogen-doped mesoporous carbons used as high-performance electrode materials in lithium-ion batteries and supercapacitors. New Journal of Chemistry, 2017, 41, 12901-12909.	1.4	19
48	The electrochemical properties of Ti0.9Zr0.2Mn1.5Cr0.3V0.3–xwt%La0.7Mg0.25Zr0.05Ni2.975Co0.525(x=0,5,10) hydrogen storage composite electrodes. International Journal of Hydrogen Energy, 2007, 32, 1898-1904.	3.8	18
49	Effect of La partial substitution for Zr on the Structural and electrochemical properties of Ti0.17Zr0.08-xLaxV0.35Cr0.1Ni0.3 (x=0–0.04) electrode alloys. International Journal of Hydrogen Energy, 2009, 34, 7246-7252.	3.8	18
50	Effects of the Preparation Solvent on the Catalytic Properties of Cobalt–Boron Alloy for the Hydrolysis of Alkaline Sodium Borohydride. Metals, 2017, 7, 365.	1.0	18
51	Effects of Alkali Metal (Li, Na, and K) Incorporation in NH2–MIL125(Ti) on the Performance of CO2 Adsorption. Materials, 2019, 12, 844.	1.3	18
52	Changes in microstructure, solidification path and hydrogen permeability of Nb–Hf–Co alloy by adjusting Hf/Co ratio. International Journal of Hydrogen Energy, 2016, 41, 1391-1400.	3.8	17
53	Ruthenium Supported on Cobaltâ€Embedded Porous Carbon with Hollow Structure as Efficient Catalysts toward Ammoniaâ€Borane Hydrolysis for Hydrogen Production. Advanced Sustainable Systems, 2021, 5, 2100209.	2.7	17
54	Hydrogen generation from ammonia borane hydrolysis catalyzed by ruthenium nanoparticles supported on Co–Ni layered double oxides. Sustainable Energy and Fuels, 2021, 5, 2301-2312.	2.5	17

#	Article	IF	CITATIONS
55	Hydrolytic dehydrogenation of NH ₃ BH ₃ catalyzed by ruthenium nanoparticles supported on magnesium–aluminum layered double-hydroxides. RSC Advances, 2020, 10, 9996-10005.	1.7	16
56	Structure, morphology and hydrogen storage properties of composites prepared by ball milling Ti0.9Zr0.2Mn1.5Cr0.3V0.3Ti0.9Zr0.2Mn1.5Cr0.3V0.3 with La–Mg-based alloy. International Journal of Hydrogen Energy, 2007, 32, 3363-3369.	3.8	15
57	The electrochemical performances of Ti–V-based hydrogen storage composite electrodes prepared by ball milling method. International Journal of Hydrogen Energy, 2008, 33, 7471-7478.	3.8	15
58	Preparation and thermal performance of n-octadecane/expanded graphite composite phase-change materials for thermal management. Journal of Thermal Analysis and Calorimetry, 2018, 131, 81-88.	2.0	15
59	Fabrication and characterization of a novel nanoporous Co–Ni–W–B catalyst for rapid hydrogen generation. RSC Advances, 2015, 5, 163-166.	1.7	14
60	Organic carbon gel assisted-synthesis of Li _{1.2} Mn _{0.6} Ni _{0.2} O ₂ for a high-performance cathode material for Li-ion batteries. RSC Advances, 2017, 7, 1561-1566.	1.7	13
61	Improved Dehydrogenation Properties of 2LiNH2-MgH2 by Doping with Li3AlH6. Metals, 2017, 7, 34.	1.0	13
62	Enhanced thermal diffusivity and dehydrogenation of 2LiNH2MgH2 by doping with super activated carbon. International Journal of Hydrogen Energy, 2018, 43, 13975-13980.	3.8	13
63	Structure and electrochemical properties of composite electrodes synthesized by mechanical milling Ni-free TiMn2-based alloy with La-based alloys. Journal of Alloys and Compounds, 2007, 446-447, 614-619.	2.8	12
64	Electrochemical performances of cobalt-free La0.7Mg0.3Ni3.5â^'x(MnAl2)x (x=0–0.20) hydrogen storage alloy electrodes. Journal of Alloys and Compounds, 2008, 457, 90-96.	2.8	12
65	Improvement on Hydrogen Desorption Performance of Calcium Borohydride Diammoniate Doped with Transition Metal Chlorides. Journal of Physical Chemistry C, 2015, 119, 913-918.	1.5	12
66	Enhancement of the electrochemical properties of rare earth-based alloy by doping with CoZnB alloy. International Journal of Hydrogen Energy, 2015, 40, 14173-14178.	3.8	12
67	Microcalorimetric investigation of the growth of the Escherichia coli DH5α in different antibiotics. Journal of Thermal Analysis and Calorimetry, 2007, 89, 875-879.	2.0	11
68	Enhancement of the initial hydrogenation of Mg by ball milling with alkali metal amides MNH2(M = Li) Tj ETQq0	0 0 rgBT //	Overlock 10 T
69	High Performance Supercapacitor based on Polypyrrole/Melamine Formaldehyde Resin Derived Carbon Material. International Journal of Electrochemical Science, 2017, 12, 1014-1024.	0.5	11
70	Study of adsorption behaviors of meso-tetrakis (4-N-Methylpyridyl) porphine p-Toluenesulfonate at indium–tin-oxide electrode/solution interface by in-situ internal reflection spectroscopy and cyclic voltammetry. Thin Solid Films, 2009, 517, 2905-2911.	0.8	10

71	Influence of Zr Addition on Structure and Performance of Rare Earth Mg-Based Alloys as Anodes in Ni/MH Battery. Metals, 2015, 5, 565-577.	1.0	10

72Influence of boron introduction on structure and electrochemical hydrogen storage properties of
Ti–V-based alloys. Journal of Alloys and Compounds, 2015, 648, 320-325.2.89

#	Article	IF	CITATIONS
73	Guanine-Derived Nitrogen-Doped Ordered Mesoporous Carbons for Lithium-Ion Battery Anodes. ChemistrySelect, 2017, 2, 10076-10081.	0.7	9
74	Investigation on the structure and electrochemical properties of AB3-type La–Mg–Ni–Co-based hydrogen storage composites. Journal of Alloys and Compounds, 2008, 462, 392-397.	2.8	8
75	Improved hydrogen desorption properties of Li-Ca-B-N-H system catalyzed by cobalt containing species. Journal of Renewable and Sustainable Energy, 2014, 6, 013105.	0.8	8
76	Low-temperature heat capacities and thermodynamic properties of Mn3(HEDTA)2·10H2O. Journal of Thermal Analysis and Calorimetry, 2010, 102, 1155-1160.	2.0	7
77	Influences of levofloxacin salts on the metabolism of Escherichia coli by microcalorimetry. Journal of Thermal Analysis and Calorimetry, 2013, 111, 959-963.	2.0	7
78	Significantly enhanced dehydrogenation properties of calcium borohydride combined with urea. Dalton Transactions, 2014, 43, 15291-15294.	1.6	7
79	Honeycomb-like Fe/Fe ₃ C-doped porous carbon with more Fe–N _{<i>x</i>} active sites for promoting the electrocatalytic activity of oxygen reduction. Sustainable Energy and Fuels, 2021, 5, 5295-5304.	2.5	7
80	The Co-B Amorphous Alloy: A High Capacity Anode Material for an Alkaline Rechargeable Battery. Metals, 2016, 6, 269.	1.0	6
81	Enhancement of the electrochemical performance of CoB amorphous alloy through the addition of A2B7-type alloy. International Journal of Hydrogen Energy, 2016, 41, 16142-16147.	3.8	5
82	Microencapsulation of phase change materials with carbon nanotubes reinforced shell for enhancement of thermal conductivity. IOP Conference Series: Materials Science and Engineering, 2017, 182, 012015.	0.3	5
83	A facile one-pot method to prepare nitrogen and fluorine co-doped three-dimensional graphene-like materials for supercapacitors. Journal of Materials Science: Materials in Electronics, 2019, 30, 19505-19512.	1.1	5
84	In Situ Synthesis of Ruthenium Supported on Ginkgo Leaf-Derived Porous Carbon for H2 Generation from NH3BH3 Hydrolysis. Recent Patents on Materials Science, 2019, 11, 65-70.	0.5	3
85	Low Temperature Heat Capacity and Thermal Analysis of Caffeine, Theophylline and Aminophylline. Wuli Huaxue Xuebao/ Acta Physico - Chimica Sinica, 2010, 26, 2096-2102.	2.2	3
86	Preparations and characterizations of perovskite 0.80PMN–0.20PT ceramic by using a one-step calcination method. Journal of Alloys and Compounds, 2010, 497, 155-158.	2.8	2
87	Feâ€Coâ€Ni/Nitrogenâ€Doped Mesoporous Carbon Materials for Electrochemical Oxygen Reduction. ChemistrySelect, 2018, 3, 12960-12966.	0.7	2
88	Superior performance for lithium storage from an integrated composite anode consisting of SiO-based active material and current collector. Frontiers of Materials Science, 2020, 14, 243-254.	1.1	1
89	Enhanced electrochemical properties of sodiumâ€doped lithiumâ€rich manganeseâ€based cathode materials. Materialwissenschaft Und Werkstofftechnik, 2021, 52, 51-59.	0.5	1
90	Metal Amidoboranes and Their Derivatives for Hydrogen Storage. , 0, , .		0

#	Article	IF	CITATIONS
91	Li1.2Mn0.6Ni0.2O2 Cathode Material Prepared by the Ultrasonic Dispersionassisted Method. Current Mechanics and Advanced Materials, 2021, 1, 58-65.	0.1	Ο